J. COMBIN. MATH. COMBIN. COMPUT. 127b (2025) 5105--5124

Journal of Combinatorial Mathematics and Combinatorial Computing
www.combinatorialpress.com/jcmcc

Combinatorial Press

Early warning technology and optimization research on real-time perception of environmental protection risk during the construction period of power transmission and transformation projects based on image processing algorithm

Xiaohu Sun[1], Xiaofeng Chen[1], Shu Zhu[1,✉], Yanbing Wang[1], Qing Li[2]

[1] *State Grid Economic and Technological Research Institute, Beijing, 102209, China*

[2] *Hubei Anyuan Safety & Environmental Protection Technology Co., Ltd., Wuhan, Hubei, 430000, China*

ABSTRACT
The level of informationization infrastructure of the power system is constantly improving, and it is of great practical significance to carry out real-time perception and early warning of environmental risks during the construction period of the project based on image processing algorithms. This paper proposes a multi-scale parallel real-time detection algorithm based on SSD, which optimizes the network structure of SSD algorithm, combines and splices different sizes of inverted residual blocks and different types of activation functions with each other, and designs a kind of lightweight feature extraction network EPNets. Then, it proposes a lightweight parallel fusion structure, which is applied to the multi-scale prediction of the lightweight feature extraction network, and optimizes the environmental risk real-time detection speed of the algorithm. The algorithm is optimized for real-time environmental risk detection speed. A Bayesian network-based environmental risk behavior warning model is constructed to provide real-time warning for the detected risk behaviors. By comparing with the original algorithm and existing target detection algorithms, the multi-scale parallel fusion detection algorithm based on SSD proposed in this paper can maintain good detection speed with low loss degree, and its environmental protection risk identification time is only 9ms.Meanwhile, the early warning algorithm in this paper realizes the accurate early warning of the soil erosion risk in the study area through the soil erosion environmental protection risk during the construction period of transmission and transformation projects detected. It provides an objective guideline for the control of environmental protection risks and work priorities.

Keywords: SSD algorithm, lightweight feature extraction network, target detection algorithm, environmental risk warning

✉ Corresponding author.
E-mail address: zhushu9293@163.com (S. Zhu).
Received 25 February 2024; Revised 10 May 2024; Accepted 15 December 2024; Published Online 16 April 2025.
DOI: 10.61091/jcmcc127b-284

1. Introduction

Under the rapid development of the power industry, the construction scale of transmission and substation projects is also expanding, and this expansion has led to a new problem of environmental protection during construction [1-3]. Since the establishment of the first 500kV ultra-high voltage transmission project in China, the electromagnetic environment has been written into the indicators of project construction quality [4-5]. Transmission and substation projects include design, project, construction, commissioning and other links, and each of these links involves environmental protection issues. However, at this stage, China has only written the environmental assessment and completion acceptance of each link into the environmental protection regulations [6-9]. The impact of power transmission and transformation projects on the ecological environment is mostly in the planning process already exists, and the problem caused by the focus of the construction period, so it is necessary to implement environmental protection measures to monitor the construction process, to improve the overall quality of power transmission and transformation projects [10-13].

Transmission and substation engineering refers to the transmission of electrical energy from the power plant to various power consumption units, as well as the conversion of electrical energy between different voltage levels. Transmission and substation engineering occupies an important position in the power system, but at the same time there are certain risks [14-17]. The construction of power transmission and transformation projects involves a wide range of areas and many environmental impact factors, and the content and focus of its environmental supervision work is different from the general ecological projects, also different from the general industrial pollution projects [18-20]. Because the work is still in the pilot stage, its work procedures, methods, content, depth and organizational mode has not formed a unified specification. At present, environmental supervision organizations mainly take the environmental impact assessment documents and approvals of power transmission and transformation projects and design documents as the basis, and carry out the work with reference to the technical specifications of engineering supervision and soil and water conservation supervision [21-24].

Literature [25] analyzed the environmental impact factors existing in the construction process of power transmission and substation projects, put forward the monitoring method based on Internet of Things (IoT) technology, and emphasized that the synergistic development of electric power engineering construction and environmental protection is a key direction for the development of this field. Literature [26] explored the optimization mode of soil and water conservation and ecological construction based on the requirements of the development of ecologically sensitive areas in Sichuan and Chongqing regions, and explored the optimization mode of soil and water conservation and ecological construction in view of the relevant contents of the construction management of transmission and substation projects, in order to provide support for the development of the city. Literature [27] based on the status quo of ecologically fragile areas and the impact of transmission and substation projects on the ecological environment, analyzes the ecological protection and vegetation restoration mode of transmission and substation construction in ecologically fragile areas, with the aim of providing a guarantee for engineering construction and industrial development. Literature [28], based on literature review, outlines the relevant information and application status of electromagnetic environment online monitoring technology in transmission and substation projects, reveals the deficiencies in electromagnetic environment online monitoring, and looks forward to its development prospects. Literature [29] examined the impact characteristics of the Three Gorges Project on the ecosystem during the construction and operation phases, and put forward corresponding protection measures, emphasizing that the activities of building towers and power stations during the construction period, as well as monitoring and maintenance during the operation period, are the main influencing factors. Literature [30] based on the construction management requirements of transmission and substation projects in Sichuan and Chongqing regions, for the construction status of ecologically sensitive areas, examined the identification of project construction in sensitive areas and the construction evaluation system, and put forward vegetation restoration techniques to ensure the normal operation of transmission and substation projects. Literature [31] analyzes the cost of environmental protection facilities of substation projects, and proposes the method of factor influence mechanism analysis based on Pearson's method and principal component analysis, which provides reference for enterprises in improving the efficiency of environmental protection costs of projects. Literature [32] discussed the ecological environment early warning system for transmission and substation projects, which adopts the multi-objective planning algorithm and introduces an intelligent model applicable to the field of transmission and substation projects, showing the advantages of comprehensive multivariate, real-time and strong target, which provides the users with accurate information data.

In this paper, based on the improvement of the first-stage detection algorithm SSD, a multi-scale parallel fusion environmental risk real-time detection algorithm is proposed. The algorithm introduces a new h-swish activation function, depth separable convolution, inverted residual block and other structures, and proposes an efficient lightweight feature extraction network, which reduces the computational cost of the algorithm and improves the accuracy of the algorithm for environmental risk detection at the same time. Then a PF-Module structure is added to the multiple prediction scales of this lightweight feature extraction network to fuse the features in parallel, which further improves the performance of the algorithm. Based on the Bayesian network, a hierarchical warning model of chemical environmental risk behaviors that can be applied to environmental risk management is constructed. Finally, a transmission and substation project in City A is taken as the research object, and relevant experiments are carried out on a self-constructed image dataset.

2. Real-time detection of environmental risk behaviors in power transmission and transformation projects

In this paper, the multi-scale parallel fusion real-time detection algorithm MSPF-DN is proposed based on the improvement of the one-stage detection algorithm SSD. The algorithm mainly improves the SSD algorithm from two aspects: on the one hand, it introduces a new activation function h-swish, and through the combination structure of different inverted residual blocks and activation functions, it designs a more efficient and lightweight feature extraction network EPNets, which improves the detection and convergence performance of the algorithm while basically not increasing the computational complexity. On the other hand, a lightweight parallel fusion structure, PF-Module, is designed and applied to multiple prediction scales of EPNets, which further improves the accuracy of the algorithm through the parallel extraction and fusion of features.

2.1. SSD Algorithm

SSD algorithm, whose full English name is Single Shot Multi Box Detector, SSD algorithm belongs to the one-stage detection and multi box prediction methods.SSD algorithm is an end-to-end target detection algorithm that directly regresses the object category and location from a feature extraction network without resampling pixels or features for border assumptions, and it is faster than FasterR- CNN [33] and YOLO [34].

With the deepening of neural network theory research and the substantial improvement of GPU arithmetic power, the target detection technique has also become a research hotspot. The current deep learning model has become the mainstream algorithm in the field of target detection, which can be divided into two major categories: one is the two-stage target detection algorithm, which divides the detection task into two phases, first generates the candidate region, and then divides the category of the candidate region, which is typified by the R-CNN algorithms, such as R-CNN, FastR-CNN, and FasterRCNN, etc. The other is the single-stage target detection algorithm. The other class is single-stage target detection algorithms, this type of algorithms can directly generate the category probability and position coordinates of the object, more typical algorithms such as Yolo series and SSD, the classification of target detection algorithms is shown in Fig. 1.

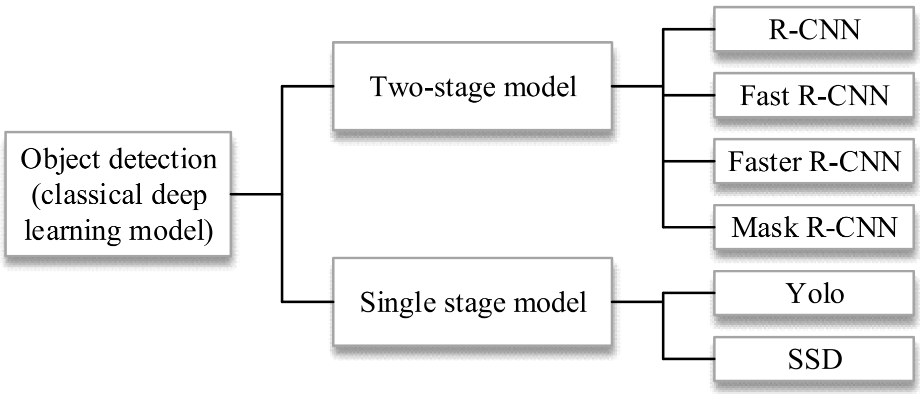

Fig.1. Classification of target detection algorithms

The feature extraction network of the SSD algorithm uses the classical VGG16 network structure with some modifications, one, the last two fully connected layers of the VGG16 network are replaced with fully convolutional layers, and two, four additional convolutional layers with decreasing scale are added after the network.

In order to ensure the balance of positive and negative samples, SSD employs a sample mining technique to sample the negative samples and ranks them in descending order according to the confidence level, where the lower the confidence level of the predicted background, the higher the error.

Since SSD regresses both the positional offsets and the category displacements of the target object, its overall objective loss function is the weighted sum of the positional and displacements losses, as shown below.

$$L(x,c,l,g)=\frac{1}{N}(L_{conf}(x,c)+aL_{loc}(x,l,g)) \quad (1)$$

Where, N is the number of matching default candidate boxes, x is the result of matching candidate boxes with real boxes, c is the category confidence, t is the prediction border, g is the real border, and α is the weight term.

In the model prediction stage, the category and confidence values are first determined according to the maximum category confidence, and the threshold is set to filter out the background prediction boxes. Then, the confidence threshold is set to filter out the boxes with lower thresholds in the prediction boxes, and the remaining prediction boxes are decoded. After decoding, the remaining prediction boxes are decoded in descending order according to the confidence, and only top-k prediction boxes are retained. Finally, the non-maximum suppression algorithm is used to filter out the large overlap in the prediction box, and the final prediction box is the detection result of the model.

2.2. h-swish activation function

The h-swish activation function is an improvement based on the swish [35] activation function, and the effect of using the swish activation function is better than using the ReLU activation function. Therefore, utilizing the swish activation function when used as an alternative to the ReLU activation function [36] in the process of building a network can significantly improve the accuracy of the neural network. However, if it is applied in an embedded environment, it is not a small computational cost, which will affect the detection speed of the network.

$$swish(x) = x \cdot \frac{1}{1+e^{-x}} \tag{2}$$

To solve the problem of computational cost, the h-swish activation function was created, which is an approximation of the swish activation function.

$$h - swish(x) = x\frac{\mathrm{Re}\,LU6(x+3)}{6} \tag{3}$$

In the process of building the network, the h-swish activation function can be used instead of the ReLU activation function to improve the detection accuracy without increasing the computational burden too much.

2.3. Deep separable convolution

Artificial neural networks were first used primarily to approximate and model biological neuronal systems, and then gradually evolved into a machine learning method. Convolutional neural networks, or CNNs, evolved from artificial neural networks and have been a landmark algorithm in computer vision in recent years.

A convolutional layer is an essential structure for a convolutional neural network, and most of the computation is done in the convolutional layer. The purpose of the convolutional layer is to extract different features by convolutional operations on the input image or feature image. For the recognition of environmental risks, the convolution kernel of the high-level neural network can extract site-specific features of environmental risks.

Assuming the dimensions of the input data are (W, H, D) and the other parameters are sliding step size S and filter size F, the dimensions of the output data (W1, H1, D1) after the pooling layer are determined by the following equation:

$$W1 = \frac{W-F}{S} + 1 \tag{4}$$

$$H1 = \frac{H-F}{S} + 1 \tag{5}$$

$$D1 = D \tag{6}$$

Usually deep learning needs to deal with more complex data types than ordinary neural networks, such as images, audio and video. Adding nonlinear activation functions to the network model allows the model to learn more complex function mappings, which can effectively prevent the model from overfitting.

In neural networks, there is a lightweight convolution structure called depth separable convolution, which decomposes the traditional convolution into a depth convolution and a 1×1 convolution, separates the channels and regions, and first considers only the channels and operates using a single-channel convolution, and then considers the regions and operates using multiple 1×1 convolutions, completing a single depth-separable convolution operation, and such an operation drastically reduces computational cost and makes the convolution operation faster.

Assuming that the input feature map F is of size $D_F \times D_F \times M$, the output feature map G is of size $D_G \times D_G \times N$, and the convolution kernel K is of size $D_k \times D_k \times M \times N$, the computation process of conventional convolution and depth-separable convolution is shown in the following equation.

$$G_{k,l,n} = \sum_{i,j,m} K_{i,j,m,n} F_{k+i-1,l+j-1,m} \tag{7}$$

$$G'_{k,l,m} = \sum_{i,j} K'_{i,j,m} F_{k+i-1,l+j-1,m} \tag{8}$$

The computational cost of conventional convolution is shown in the following equation.

$$T = D_k \times D_k \times M \times N \times D_F \times D_F \tag{9}$$

The computational cost of the depth separable convolution is shown in the following equation.

$$K = D_k \times D_k \times M \times D_F \times D_F + M \times N \times D_F \times D_F \tag{10}$$

The computational cost ratio of deep separable convolution to conventional convolution is shown in the following equation.

$$\frac{K}{T} = \frac{1}{N} + \frac{1}{D_k^2} < 1 \tag{11}$$

Deeply separable convolution significantly reduces the computational cost compared to conventional convolution.

2.4. Inverted residual blocks and linear bottlenecks

Residual blocks have been shown to help improve accuracy, so the inverted residual block borrows the idea of the residual module in ResNet and introduces the shortcut structure. The input first undergoes a 1×1 convolution for dimensionality compression, then a 3×3 convolution is utilized for feature extraction, and finally a 1×1 convolutional layer is used for dimensionality upgrading, which is done to improve the overall computational efficiency of the residual block. The process of inverting the residual block first goes through 1×1 convolutional upscaling for channel expansion, then uses 3×3 depth-separable convolution for feature extraction, and finally compresses the number of channels back with 1×1 convolution, which is exactly the opposite of the operation of the standard ResNet module.

It can be seen that in the feature extraction stage, the residual block uses traditional convolution, and the inverted residual block uses depth-separable convolution, and the use of depth-separable convolution greatly reduces the computational cost, but the performance of depth-separable convolution is worse in low dimensions, so in the design of the inverted residual block, the convolution should be upgraded before using depth-separable convolution, which in turn improves the accuracy.

2.5. Improved SSD-based multi-scale parallel fusion real-time detection algorithm

The multiscale parallel fusion real-time detection algorithm MSPF-DN introduces the activation function h-swish and improves the SSD algorithm. In order to balance both accuracy and speed, depth-separable convolution is used in the designed network to make it as lightweight as possible. First, a lightweight feature extraction network EPNets is designed to speed up the detection. Second, a lightweight parallel fusion structure, PF-Module, is designed to further enhance the detection. Subsequently, the multi-scale feature maps output from the PF-Module structure are fed into the detection and classifier, and finally the final detection results are obtained by non-maximum suppression.

In this paper, the feature extraction network EPNets is improved with reference to the MobilenetV2 network. Due to the requirement of lightweight, depth separable convolution is used extensively in the network, and two kinds of towers are used for the use of inverted residual blocks: 3×3 inverted residual blocks are paired with ReLU activation function, and 5×5 inverted residual blocks are paired with h-swish activation function.

The feature extraction network EPNets completes the first step of feature extraction, and due to the extensive use of depth-separable convolution and inverted residual blocks, although it achieves sufficient lightness, it inevitably loses some of the general features. In order to further extract more features and improve the accuracy, this paper designs a lightweight parallel fusion structure PF-Module, the structure is shown in Fig. 2.

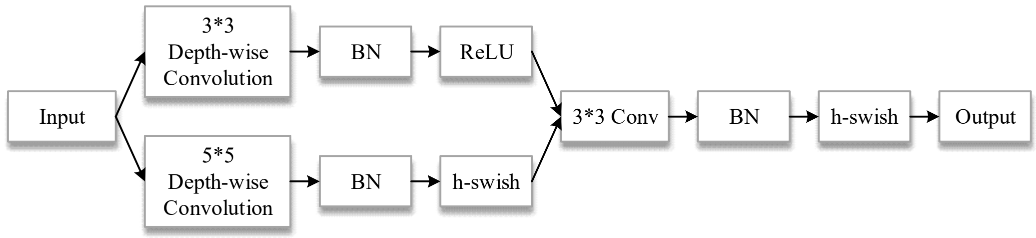

Fig.2. Structure of PF-Module

Instead of the previous single-path processing, the input feature maps do their operations in two separate branches: one branch uses a 3×3 pairing of a depth-separable convolution and a ReLU activation function. The other branch uses a 5×5 pairing of depth-separable convolution and h-swish activation function. The feature maps obtained from the two branches are summed and fused, and a parallel fused feature map is obtained by using a 3×3 pairing of conventional convolution and h-swish activation function, filtering redundant information, and outputting.

3. Early warning model for environmental risks during the construction period of power transmission and transformation projects

3.1. Bayesian network structure building

Bayesian networks, as a tool for dealing with systematic uncertainty, can effectively represent uncertain knowledge as well as causal links between learning variables through probability theory. Through the model constructed on the basis of Bayesian network, the impact of uncertainties on the outcome can be analyzed in detail and the interactions among nodes are fully considered, so it is widely used in the field of assisted decision-making. The structure and parameter settings of Bayesian networks mainly rely on expert knowledge or in-depth analysis of relevant data to determine. Once these structures and parameters are determined, the algorithmic reasoning can be executed.

A Bayesian network can be represented by the binary group $B=(G,\theta)$: where G denotes the Bayesian network structure, the underlying structure of the Bayesian network is a directed acyclic graph, which can be denoted as $G=(V,A)$, V is the node variable in the directed acyclic graph, i.e., $V=\{V_1,V_2,...,V_n\}(n\geq 1)$, A is denoted as a collection of arcs in the Bayesian network; θ is denoted as the parameters of the Bayesian network, which can be denoted as $P(V_i \mid pa(V_i))$, and is used to characterize conditional probabilistic relationships among nodes. (V_i,V_j) a directed edge in the Bayesian network, V_i pointing to V_j. The parent node of node V_i can be represented by $pa(V_i)$ and non-descendant nodes are represented using $A(V_i)$. When the parent node $pa(V_i)$ is given, V_i is conditionally independent from $A(V_i)$, i.e:

$$P(V_i \mid pa(V_i), A(V_i)) = P(V_i \mid pa(V_i)) \tag{12}$$

The joint probability distribution of the Bayesian network is shown in the public following equation.

$$P(V_1,V_2,...,V_k)=\prod_{i=1}^{k} P(V_i \mid V_{i-1},V_{i-2},...,V_1)=\prod_{i=1}^{k} P(V_i \mid pa(V_1)) \tag{13}$$

Bayesian network modeling usually consists of three main steps. First, the factors affecting the event and their possible states are identified; these factors are usually set up as nodes in a Bayesian network, and a different state of each node will have a different effect on the other nodes. This step can be done based on expert experience when there is a lack of relevant case support or when there is insufficient data. Next, the Bayesian network is built based on the nodes and states identified in the first step. In the process of building the Bayesian network, it is necessary to specify the interdependencies between the nodes, which are represented by directed edges and point from the parent to the children. Finally, the conditional probability distribution of each node is determined so that the interactions between nodes can be more accurately described, and the determination of these conditional probabilities is often based on real data or expert knowledge.

In this paper, a Bayesian network with four nodes for hierarchical early warning of environmental risk behaviors during the construction period of transmission and substation projects is established by combining previous research and expert experience in order to analyze the probability of occurrence of environmental risk behaviors during the construction period of transmission and substation projects, and to provide managers with reasonable and effective information on environmental risks. The overall Bayesian model of environmental risk behavior grading and early warning during the construction period of transmission and substation projects consists of three modules: signal module, judgment module and early warning module.

The early warning module includes only one node, "Risk level of environmental protection risk behavior during the construction period of power transmission and transformation project", which reflects the risk level probability of environmental protection risk behavior in the current scenario. This node is jointly determined by four nodes of the judgment module, namely, "Identification result of vegetation destruction behavior", "identification result of soil erosion behavior", "identification result of electromagnetic radiation" and "identification result of noise pollution behavior". The early warning of environmental protection risk behavior risk level is shown in Table 1. S1 and S2 are in the safe zone, when the environmental risk behavior is identified as S3 level, there is an environmental risk warning, and relevant intervention measures must be taken.

Table 1. Environmental warning

Node	Node status and description
Vegetation damage behavior	S1: Vegetation coverage is 50% to 70%
	S2: Vegetation coverage is 30% to 50%
	S3: Vegetation coverage is less than 30%
Soil erosion behavior	S1: The total erosion is less than 1000t
	S2: The total amount of erosion is 1000t-2000t
	S3: The total amount of erosion is greater than 2000t
Electromagnetic radiation identification	S1: The high frequency radiation is less than 10 milliwatts per square centimeter, and the low frequency radiation is less than 10 volts per meter
	S2: The high frequency radiation is less than 40 milliwatts per square centimeter, and the low frequency radiation is less than 25 volts per meter
	S3: High frequency radiation is greater than 40 milliwatts per square centimeter, and low frequency radiation is greater than 25 volt ampere per meter
Noise pollution behavior	S1: Decibel range 30 to 59
	S2: Decibel range 60 to 89
	S3: The decibel range is greater than 89

3.2. Bayesian network node probability distribution setting

In this paper, the probability distribution of partial nodes in the judgment module and the probability distribution are determined based on the precision rate P and the recall rate R of the model. The probability distributions of the partial nodes were calculated by distributing a questionnaire to the experts and using the Dempster-Shafer (D-S) theory of evidence approach.

The D-S theory of evidence theory is a set of theoretical frameworks for dealing with inexact inferences, which has a wide range of applications and is particularly suitable for scenarios such as dealing with uncertainty reasoning, risk assessment, and providing decision support. Based on the available evidence and knowledge, this theory is capable of reasoning and analyzing ambiguous information. In addition, D-S theory provides a systematic set of synthesis methods that allow multiple pieces of evidence to be synthesized through specific formulas, generating underlying plausibility while ensuring that these synthesized results retain their original properties.

The D-S evidence theory defines the identification framework and the quality function, let θ be the identification framework, then the quality function has to satisfy the following conditions:

$$\begin{cases} m(\varnothing)=0 \\ \sum_{A\subset\theta} m(A)=1 \end{cases} \tag{14}$$

where $m(A)$ is the quality function of event A and represents the level of trust in A. D-S evidence theory outputs a new trust assignment by employing a multi-source data synthesis rule that synthesizes the underlying trust assignments from multiple data sources.

$$(m_1 \oplus m_2 \oplus \cdots \oplus m_n)(A) = \begin{cases} 0, A=\varnothing \\ \dfrac{1}{K} \sum_{A_1\cap A_2\cap\cdots\cap A_n=A} m_1(A_1)\cdot m_2(A_2)\cdots m_n(A_n) \end{cases} \tag{15}$$

where $m_1, m_2, \ldots, m_n$ is the basic confidence distribution function of the identification framework θ, n is the total number of quality functions, where K is the normalization factor, and K is calculated as shown in Equation (16).

$$K = \sum_{A_1 \cap A_2 \cap \cdots \cap A_n \neq \varnothing} m_1(A_1) \cdot m_2(A_2) \cdots m_n(A_n) = 1 - \sum_{A_1 \cap A_2 \cap \cdots \cap A_n = \varnothing} m_1(A_1) \cdot m_2(A_2) \cdots m_n(A_n) \tag{16}$$

4. Effectiveness of environmental risk detection during the construction period of power transmission and transformation projects

In the experiment, the proposed model parameters are first initialized using the weights of the classical network, and then 2000 sheets are randomly selected as the training set, 500 sheets are randomly selected as the validation set, and the remaining 1500 sheets are used as the test set from the environmental protection risk dataset during the construction period of transmission and substation projects. The setting of hyperparameters in the training process is very important, and this paper chooses the empirical values as the initial values of hyperparameters. In this case, the learning rate is set to 0.0015, batch_size is set to 16, and epoch is set to 600. The accuracy and loss rate of the training process are shown in Figures 3 and 4, respectively. During the model training phase, the error change is less than 0.05 by about the 300th iteration, and the change is smoother. Finally, a test sample set is used to test the trained model, the original data set of a transmission and substation project in the construction period of different environmental risk distribution area shown in Figure 5, Figure 6 shows the detection method of this paper on the identification of environmental risks, the proposed detection algorithm based on the improvement of the SSD is able to achieve effective identification of the destruction of vegetation, soil erosion, electromagnetic radiation of the three different types of environmental risks, where the environmental risk of the destruction of vegetation in a geographical area is identified as soil erosion risk. A geographical area of vegetation destruction type of environmental protection risk identified as soil erosion risk, the reason may be that the risk of destruction of vegetation and soil erosion has certain similarities, after the destruction of vegetation to a certain extent will lead to soil erosion, on the whole, this paper's detection algorithm recognition effect is better.

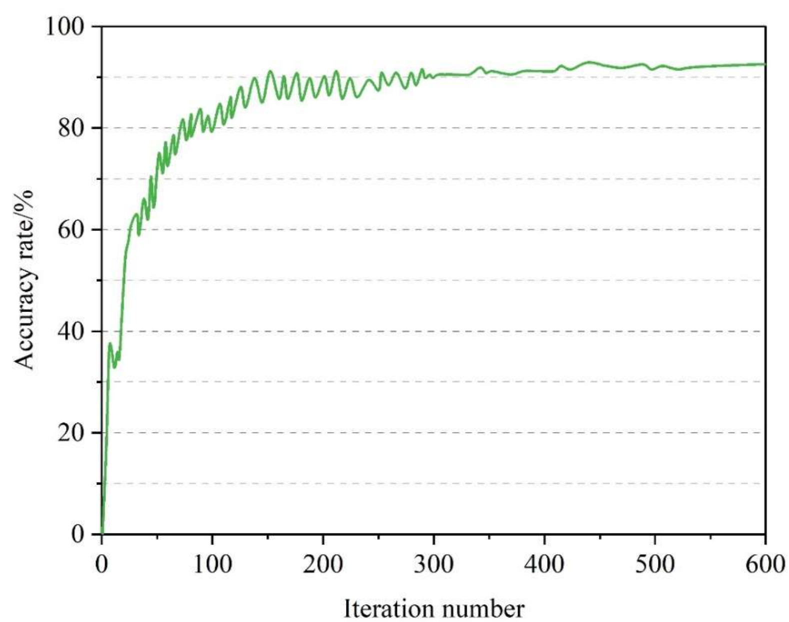

Fig. 3. Accuracy of training process

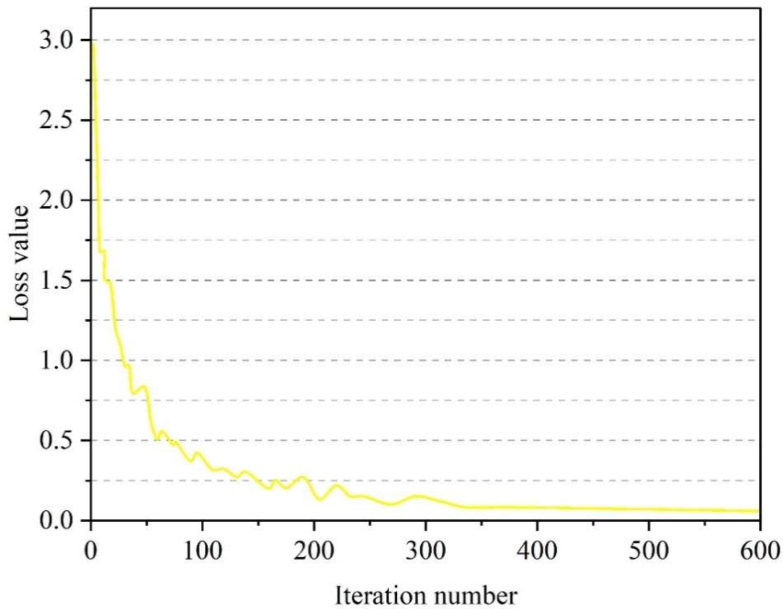

Fig. 4. The loss rate of the training process

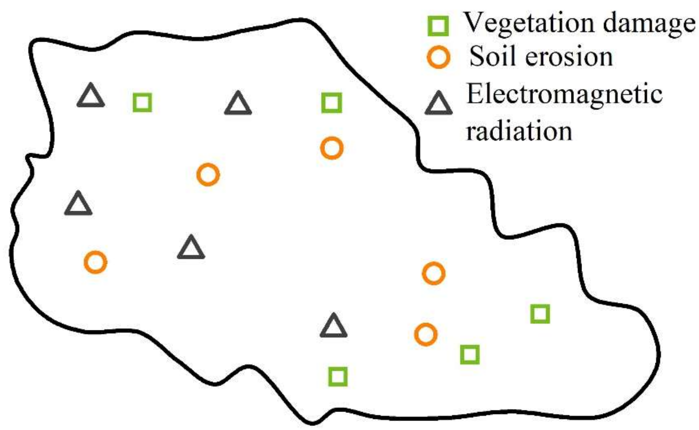

Fig. 5. Different environmental risk distribution area

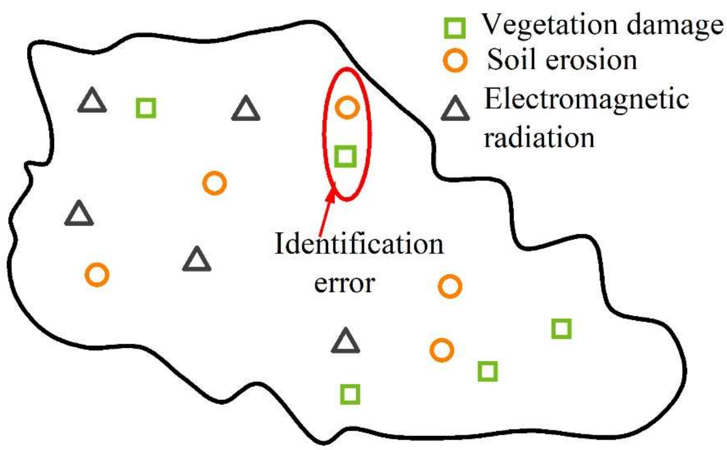

Fig. 6. This paper alerts the effect of environmental risk

In order to further validate the advantages of the proposed method in environmental risk identification, the proposed algorithm and commonly used deep learning algorithms are tested and compared on the same dataset, including four classical one-stage and two-stage target detection algorithms, namely, YOLO, original SSD, Faster-RCNN and Mask-RCNN, and the results are shown in Table 2.

The different algorithms are compared in terms of four aspects: mAP, recognition speed, model size, and model training time, respectively. From the table, it can be seen that One-stage class algorithms are significantly better than Two-stage class algorithms in terms of recognition speed, model size and training time. And the Two-stage class algorithm is significantly better than the One-stage class algorithm in terms of recognition accuracy. Among them, the algorithm proposed in this paper is slightly inferior to the Two-stage class algorithm in terms of accuracy, but in terms of comprehensive ability, it is most suitable for deployment to realize the task of detecting and identifying environmental risk behaviors during the construction period of transmission and substation projects, and the recognition speed of this paper's algorithm is only 9ms, which is capable of identifying environmental risks and their localization in a fast and high-precision manner.

Table 2. Differences in the identification results of different algorithms

Algorithm	mAP/%	ms/piece	Model size	Training time/ms
YOLO	88.5	24	199	13
Primordial SSD	92.1	43	234	15
Faster-RCNN	94.6	49	745	33
Mask-RCNN	97.5	49	546	38
This algorithm	92.9	35	25	9

In order to judge the performance of the improved model more accurately, the epoch is set to 10000, and the classification loss function values and location loss values of the original SSD model and the improved SSD model are plotted as shown in Figures 7-Figures 10, respectively. It can be intuitively observed that the improved SSD model has a higher detection accuracy, and its classification loss and location loss finally converge at 0.06 and 0.08, which are smaller than those of the original SSD model, and can more accurately detect the environmental risk categories of concern.

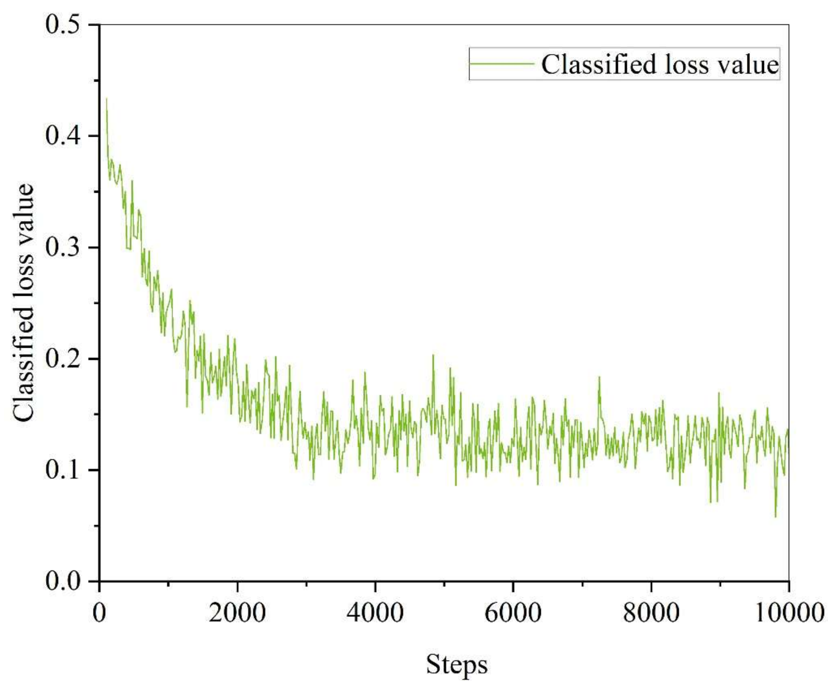

Fig. 7. Original SSD model classification loss function value

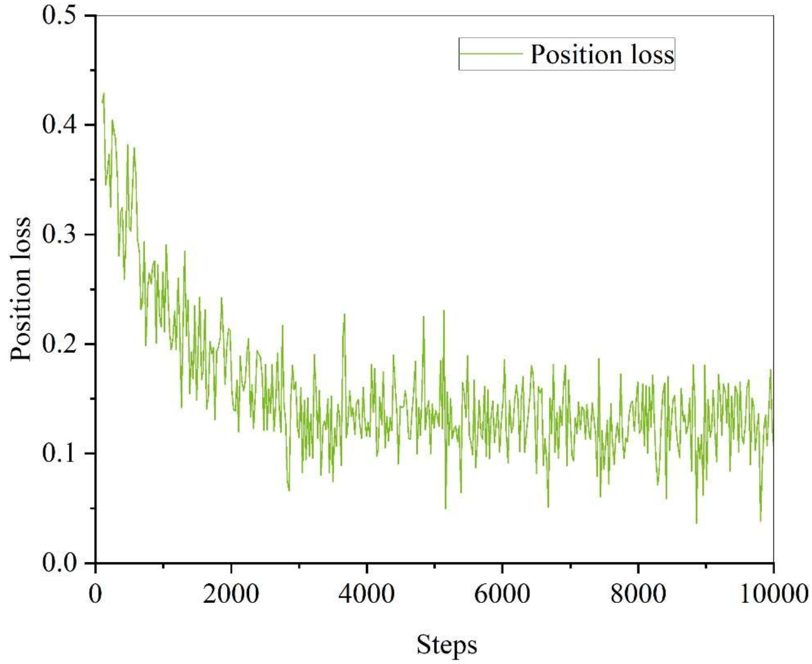

Fig. 8. Original SSD model location loss

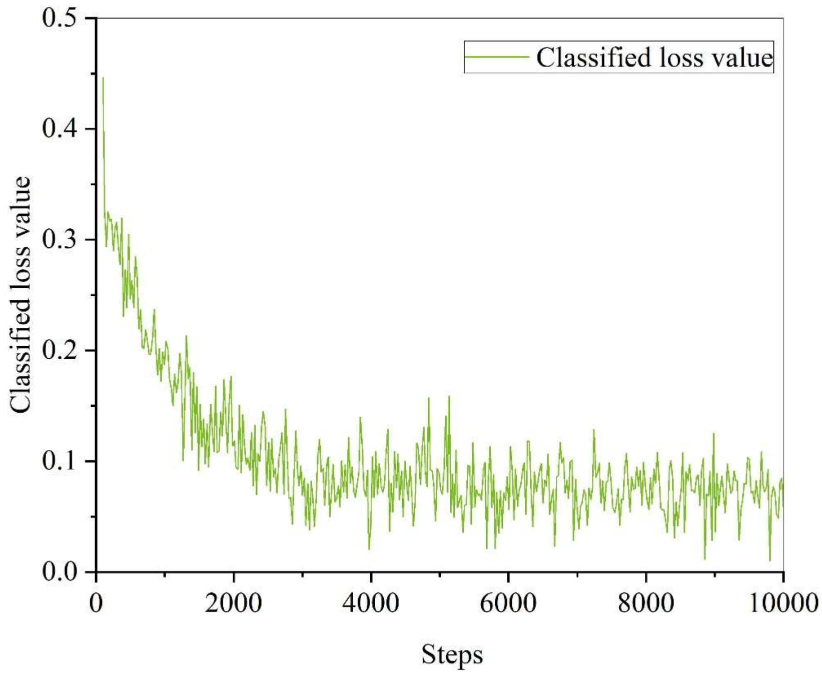

Fig. 9. Improved SSD model classification loss function value

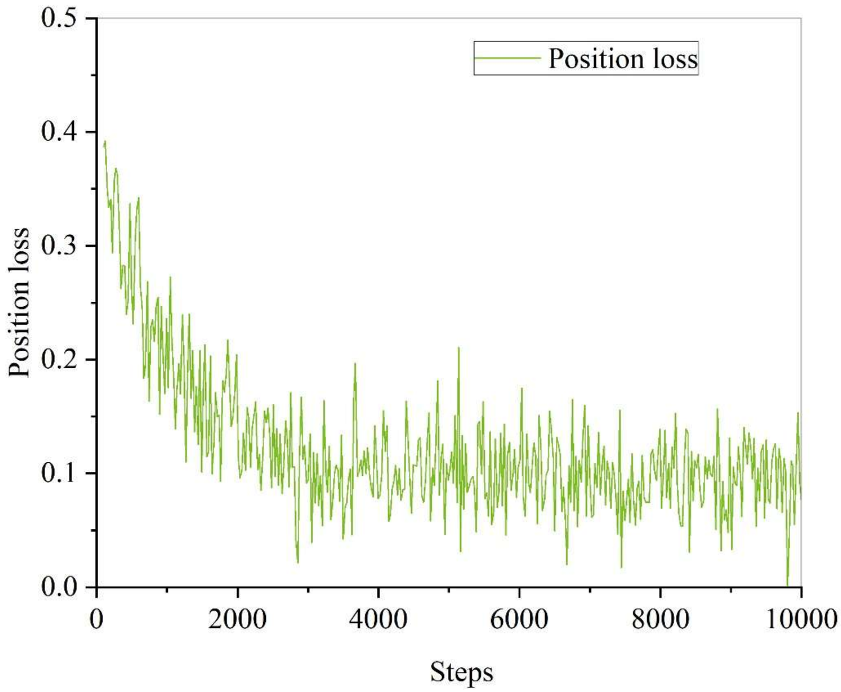

Fig. 10. Improved SSD model location loss

5. Analysis of the effectiveness of early warning on environmental risk behaviors

In order to verify the feasibility of the proposed real-time environmental risk perception and early warning method for transmission and substation projects and apply it to the soil erosion risk monitoring task, a 500kV transmission and substation project in city A was taken as the study area, and seven pictures taken at different heights were selected as the data source to validate the effectiveness of the environmental risk monitoring. The seven different heights of the pictures taken at 110, 120, 130, 140, 150, 160 and 170m, and the seven monitoring results of disturbed land area and abandoned land area during construction were obtained as shown in Figs. 11 and 12, respectively, 140, 150, 160 and 170 m. The results of the seven times of disturbed land area and abandoned land area during construction are shown in Fig. 11 and Fig. 12, respectively.

As can be seen from Fig. 11, the monitoring height of 170m is the closest to the measured value, and its relative deviation is only 0.35%, which is the smallest monitoring error among the seven tests. Overall, the deviation of the seven monitoring results ranged from 0.35% to 0.48%, indicating that the results of the disturbed land area obtained by the proposed environmental risk monitoring algorithm are more accurate.

The monitoring heights of 140 and 150 m are the closest to the actual amount of land disposal of the substation project. The relative deviation was -1.98% for the 150m height and 1.65% for the 140m height. The other monitoring heights yielded slightly larger disposal quantities than the measured values of the project, but the overall deviation was controlled within 12%. Based on the results of the land area disturbed by the project and the amount of soil disposed of at different monitoring altitudes, the study was carried out at a flight altitude of 140 m. The results were summarized as follows.

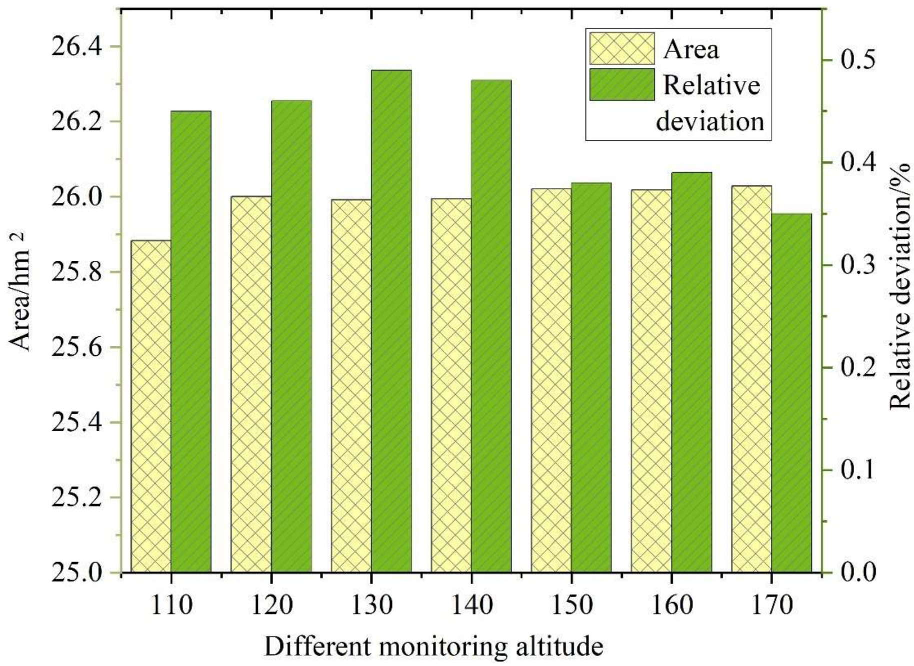

Fig. 11. Disturbed land area

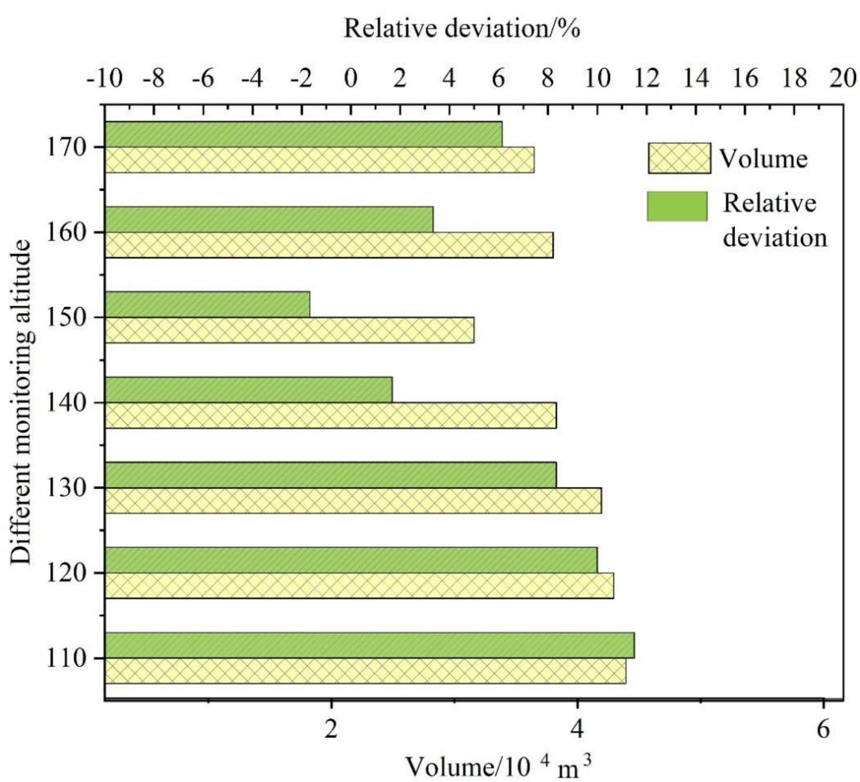

Fig. 12. Soil area monitoring results

The study set an algorithm monitoring height of 140m for environmental risk monitoring of soil erosion in the study area. The actual monitoring scope is shown in Table 3. The permanently occupied station site and approach road area covers the most area, which is 11.15hm^2.

Table 3. project monitoring scope statistics

Project	Cover type/hm^2	Area

		Woodland	Grass	Transport land	Land and water conservancy facilities	meter
Permanent cover	Site and inbound road area	6.35	2.64	0.18	1.98	11.15
	The permanent floor of the tower	1.09	0.23	0.00	0.00	1.32
	Microscope	7.44	2.87	0.18	1.98	12.47
Temporary cover	Construction camp	0.00	0.29	0.00	0.00	0.29
	Kentucky space	6.03	1.46	0.00	0.00	7.49
	Stretch field	0.00	2.18	0.00	0.00	2.18
	Construction road	0.69	0.00	2.65	0.00	3.34
	Cross construction site	0.00	0.35	0.00	0.00	0.35
	Microscope	6.72	4.28	2.65	0.00	13.65
Tot		14.16	7.15	2.83	1.98	26.12

The project's soil and water conservation monitoring area is 26.12hm^2, including 12.47hm^2 of permanent occupation and 13.65hm^2 of temporary land. The study utilizes the early warning algorithm based on Bayesian network proposed in the previous paper to monitor the environmental risk of seven projects in the permanent and temporary land occupied by the substation and transmission line. Among them, the monitoring period is from January 2023 to December 2023 during the construction period and from January 2024 to December 2024 during the forest and grass restoration period. According to the early warning algorithm based on Bayesian network in this paper, the amount of soil erosion of the project obtained by further calculation and analysis is shown in Table 4.

The total amount of soil erosion during the construction period is 1257.00t, and the amount of new soil erosion is 1159.00t. It can be seen that the soil erosion in the study area is at the S2 level of the environmental risk warning of soil erosion, which can be naturally restored during the recovery period without intervention. Compared with the amount of soil erosion in the construction period, the total amount of soil erosion in the natural recovery period is reduced by 73.59%, and the amount of new soil erosion is reduced by 85.50%. The soil erosion in the construction and natural recovery periods mainly occurs in the station site and the inlet road area, which is the focus of soil erosion prevention and control, as well as the focus of environmental protection risk monitoring. Factors affecting soil erosion mainly include the nature of precipitation characteristics (amount, intensity and time of rainfall, etc.), geographic location, geological features, composition of the ground components, plant species, vegetation coverage, the distribution of engineering protection facilities, etc., of which man-made disturbance of the ground surface is the main cause of soil erosion. Therefore, in the process of carrying out the construction of power transmission and transformation projects, the managers should pay attention to the measures such as temporary blocking and vegetation restoration, in order to achieve the reduction of soil and water erosion and reduce the risk of environmental protection.

Table 4. Water and water loss monitoring results

Control partition	Monitoring period	Background value F/ t·(km²·a)-1	Erosion modulus F/ t·(km²·a)-1	Area/hm²	Total soil erosion/t	New soil and water loss/t
Address and inbound road	Construction period	500.00	8000.00	11.15	1100.00	1040.00
	Natural recovery period	500.00	1200.00	4.58	90.00	45.00
Construction camp	Construction period	500.00	4200.00	0.29	11.00	10.00
	Natural recovery period	500.00	1000.00	0.29	6.00	4.00
Kentucky	Construction period	500.00	1930.00	8.81	83.00	61.00
	Natural recovery period	500.00	1000.00	8.77	175.00	85.00
Stretch field	Construction period	500.00	1500.00	2.18	18.00	13.00
	Natural recovery period	500.00	1200.00	2.18	42.00	21.00
Construction road	Construction period	500.00	2400.00	3.34	41.00	32.00
	Natural recovery period	500.00	1100.00	0.78	14.00	9.00
Cross construction site	Construction period	500.00	1500.00	0.35	4.00	3.00
	Natural recovery period	500.00	1000.00	0.35	5.00	4.00
Tot	Construction period	-	-	26.12	1257.00	1159.00
	Natural recovery period	-	-	16.95	332.00	168.00
	Tot	-	-	-	1589.00	1327.00

6. Conclusion

This paper proposes a multi-scale parallel detection algorithm based on SSD, which is applied to the environmental risk detection during the construction period of transmission and substation projects and combined with Bayesian network to realize early warning.

The optimization algorithm in this paper solves the problem of lower detection accuracy and detection speed of traditional image processing algorithms on the environmental risk image dataset during the construction period of transmission and substation projects. The optimization algorithm introduces the activation function h-swish, and depth separable convolution, which improves the detection accuracy of the algorithm. Experiments show that the algorithm in this paper has excellent detection accuracy in the identification of different types of environmental risks during the construction period of transmission and substation lines, with a lower loss rate than the original algorithm, and at the same time, it has a faster real-time detection speed, and the speed of the algorithm for environmental risk identification is only 9ms.

In the practical application of the early warning algorithm based on Bayesian network in this paper, the algorithm realizes the real-time perception and early warning of environmental protection risk of soil erosion during the construction period of transmission and substation project, and identifies the soil erosion risk of the study area as S2 level, and the total amount of soil erosion during the construction period of the transmission and substation project is 1,257.00t, and the total amount of soil erosion during the period of natural restoration is reduced by 73.59% compared with that of the construction period. It shows that the construction period of the transmission and substation project is the main influence time period of the overall environmental protection risk of the transmission and substation project, in order to reduce the environmental pollution brought by the environmental protection risk at the later stage, the environmental protection risk warning and treatment work during the construction period of the transmission and substation project should be emphasized. The results of this paper provide technical support and research direction for the green construction and environmental optimization of power transmission and transformation projects.

Funding

The paper is funded by the State Grid Corporation of China's technology project: "Real time perception and early warning technology for environmental risks during the construction period of power transmission and transformation projects and its application research (project code: 5200-202456108A-1-1-ZN).

References

[1] Yang, J., Bian, R., Wang, T., Huang, J., & Wang, S. (2024). Design Capability Evaluation and System Development for Power Transmission and Transformation Engineering. In E3S Web of Conferences (Vol. 520, p. 03015). EDP Sciences.

[2] Li, H., Hu, W. L., Shi, J., Yang, J. Y., Ge, Y., Zhu, L., ... & Pu, D. (2019). Accurate investment forecasting of power transmission and transformation project based on BP neural network and regression analysis. In Application of Intelligent Systems in Multi-modal Information Analytics (pp. 456-465). Springer International Publishing.

[3] Chen, B., Liu, Q., Zeng, C., Yin, C., Wang, Z., Shu, H., & Liao, W. (2024). Analysis Of the Influence Mechanism of Power Market Reform Affecting the Power Transmission and Transformation Construction Projects Under the DB Mode. Highlights in Science, Engineering and Technology, 81, 663-671.

[4] Sun, K., Xu, K., Zheng, Z. M., Ding, X. Y., Sun, K., Chen, H. W., & Jiang, Q. Y. (2014). Power transmission and transformation project establishing and decision-making based on ASU-MOPSO algorithm. Applied Mechanics and Materials, 521, 521-529.

[5] Wang, Y., Chen, H., Zhao, S., Fan, L., Xin, C., Jiang, X., & Yao, F. (2024). Benefit Evaluation of Carbon Reduction in Power Transmission and Transformation Projects Based on the Modified TOPSIS-RSR Method. Energies, 17(12), 2988.

[6] Liu, Q., Yin, C., & Chen, B. (2021). Study on schedule risk assessment of power transmission and transformation project based on improved risk chain. In IOP Conference Series: Earth and Environmental Science (Vol. 621, No. 1, p. 012018). IOP Publishing.

[7] Zhou, X., Fan, S., Sun, H., Tang, L., & Ma, F. (2021). Practices of environmental protection, technological innovation, economic promotion and social equity in hydropower development: A case study of cascade hydropower exploitation in China's Dadu River basin. Clean Technologies and Environmental Policy, 1-15.

[8] Zhang, J., & Lin, T. (2023). Analysis on the construction and application of comprehensive evaluation index system of construction quality of power transmission and transformation project. Advances in

Engineering Technology Research, 8(1), 413-413.

[9] Wang, Y. (2022). Research on Operation Safety of Power Transmission and Transformation Equipment in Wind Power Plant. International Journal of Frontiers in Engineering Technology, 4(6).

[10] Zhao, X., Guo, L., Li, Y., & Ni, T. (2021). Study on risk management and control of power transmission and transformation project in power grid. In E3S web of conferences (Vol. 253, p. 02025). EDP Sciences.

[11] Wang, Z., Hu, L., Huang, X., Tan, J., & Ye, K. (2024). Carbon emissions of power transmission and transformation projects in the whole life cycle for smart sustainable energy systems. Scientific Reports, 14(1), 3812.

[12] Zhi, Y., Zhou, Y., Zheng, Y., Liu, Q., & Yan, L. (2023). Discussion on feature enhancement technology of audit object of power transmission and transformation project settlement based on remote sensing technology. Advances in Engineering Technology Research, 8(1), 359-359.

[13] Bian, G. (2023). Research on Safety Risk Identification and Control Strategy of Power Transmission and Transformation Project Construction Site. Journal of Electrotechnology, Electrical Engineering and Management, 6(4), 73-78.

[14] Ding, Y., Zhang, X., Zhou, L., & Xu, C. (2022). Investment Risk Assessment of EPC Power Transmission and Transformation Projects under New Energy Grid Connection Based on the Owner's Perspective. Mathematical Problems in Engineering, 2022(1), 2258938.

[15] Zhang, Z., Yang, H., Xu, L., Li, X., Liu, Q., & Yu, W. (2022). Research progress of vegetation restoration technology in power transmission and transformation project. Advances in Engineering Technology Research, 1(3), 104-104.

[16] Chen, X., & Ou, Y. (2023). Carbon emission accounting for power transmission and transformation equipment: An extended life cycle approach. Energy Reports, 10, 1369-1378.

[17] Wang, C., Gao, X., & Long, H. (2025). Carbon Emission Accounting for 220 kV Transmission and Transformation Projects Based on a Whole Life Cycle Improvement Method. Energies, 18(4), 912.

[18] Chen, F., Yang, K., Wang, L., Zhang, Y., & Liu, H. (2022). Comprehensive evaluation of power transmission and transformation project based on electric power big data. Energy Reports, 8, 733-741.

[19] Xin, J., ShangKe, L., YanLi, X., & Ye, W. (2021). Prediction model for cost data of a power transmission and transformation project based on Pearson correlation coefficient–IPSO–ELM. Clean Energy, 5(4), 756-764.

[20] Kang, Z. (2022, November). Transmission and Transformation Engineering Management System Based on Distributed Load Balancing. In International conference on Advances in Materials and Manufacturing (pp. 645-655). Singapore: Springer Nature Singapore.

[21] Zhao, H., & Li, N. (2015). Risk evaluation of a UHV power transmission construction project based on a cloud model and FCE method for sustainability. Sustainability, 7(3), 2885-2914.

[22] Zhao, J., & Yue, X. (2020). Condition monitoring of power transmission and transformation equipment based on industrial internet of things technology. Computer Communications, 157, 204-212.

[23] Zhao, S., Chen, H., Jia, C., Wang, Y., Xin, C., & Jiang, X. (2024). Comprehensive Evaluation and Scheme Optimization for Power Transmission and Transformation Projects with the Adoption of Carbon Reduction Technologies. Energies, 17(3), 598.

[24] Yang, F., Chen, F., Zhao, C., Li, J., & Kang, J. (2023). Analysis and Prediction of Differential Operation and Maintenance Cost of Power Transmission and Transformation. Procedia Computer Science, 228, 1277-1286.

[25] Zhai, X., & Cheng, X. (2020). Environmental protection requirements of power transmission and

transformation project construction based on Internet of Things technology and its change trend analysis. In IOP Conference Series: Materials Science and Engineering (Vol. 740, No. 1, p. 012144). IOP Publishing.

[26] Zhang, W., Fan, R., Zeng, W., Yu, W., Li, G., Li, J., ... & Xu, L. (2023). The optimization model of soil and water conservation ecological construction for power transmission and transformation projects in ecologically sensitive areas in Sichuan and Chongqing area in the new era is analyzed. Advances in Economics and Management Research, 7(1), 353-353.

[27] Hong, Q., Chen, X., Xu, L., Han, L., Qian, Y., & Wang, X. (2023). Study on ecological protection and vegetation restoration model of power transmission and transformation project construction in typical ecologically fragile areas in western China in the new period. Advances in Engineering Technology Research, 7(1), 478-478.

[28] Peiming, L., Jian, Z., Jun, X., Wenjin, W., & Xiaoyang, G. (2019). Research Progress of On-line Monitoring Technology for Electromagnetic Environment of Power Transmission and Transformation Projects. Meteorological and Environmental Research, 10(6), 67-71.

[29] Mo, H., Liang, D., Wen, W., Su, B., Hong, Q., Chen, F., & Zhao, Y. (2019, February). Interference pathway of power transmission and transformation project on ecosystem. In IOP Conference Series: Earth and Environmental Science (Vol. 227, No. 6, p. 062032). IOP Publishing.

[30] Yang, D., Du, S., Zhang, W., Fan, R., Liu, Q., Zeng, W., ... & Li, J. (2023). Study on vegetation restoration technology in ecologically sensitive area of power transmission and transformation project in Sichuan-Chongqing area. Advances in Education, Humanities and Social Science Research, 8(1), 83-83.

[31] Yu, X., Yu, M., Yang, X., & Liu, F. (2022). Analysis and research on the influencing factors and influencing mechanism of environmental protection facilities in power transmission and transformation project. In Energy Revolution and Chemical Research (pp. 93-98). CRC Press.

[32] Lv, M., & Tong, J. (2022, December). Research on Ecological Environment Early Warning System of Power Transmission and Transformation Project Based on Multi-objective Programming Algorithm. In International Conference on Big Data Analytics for Cyber-Physical System in Smart City (pp. 301-308). Singapore: Springer Nature Singapore.

[33] Weijie Liu,Jie Hu & Jin Qi. (2025). Resistance Spot Welding Defect Detection Based on Visual Inspection: Improved Faster R-CNN Model. Machines(1),33-33.

[34] Hanlong Yang,Lujie Wang,Yue Pan & Jin Jian Chen. (2025). A teacher-student framework leveraging large vision model for data pre-annotation and YOLO for tunnel lining multiple defects instance segmentation. Journal of Industrial Information Integration100790-100790.

[35] Nawaz Marriam,Saleem Sumera,Masood Momina,Rashid Junaid & Nazir Tahira. (2024). COVID-ECG-RSNet: COVID-19 classification from ECG images using swish-based improved ResNet model. Biomedical Signal Processing and Control105801-.

[36] Mohammad Mehdi Dehghani,Khashayar Mehrany & Mohammad Memarian. (2024). All-optical multi-wavelength-channel ReLU activation function.. Optics express(22),39160-39176.